Published in final edited form as:
Dev Biol. 2009 May 15; 329(2): 201–211. doi:10.1016/j.ydbio.2009.02.030.

Lipocalin signaling controls unicellular tube development in the *Caenorhabditis elegans* excretory system

Craig E. Stone[a], **David H. Hall**[b], and **Meera V. Sundaram**[a,*]

[a]Department of Genetics, University of Pennsylvania School of Medicine, Philadelphia, PA 19104, USA

[b]Department of Neuroscience, Center for C. elegans Anatomy, Albert Einstein College of Medicine, Bronx, NY 10461, USA

Abstract

Unicellular tubes or capillaries composed of individual cells with a hollow lumen perform important physiological functions including fluid or gas transport and exchange. These tubes are thought to build intracellular lumina by polarized trafficking of apical membrane components, but the molecular signals that promote luminal growth and luminal connectivity between cells are poorly understood. Here we show that the lipocalin LPR-1 is required for luminal connectivity between two unicellular tubes in the *Caenorhabditis elegans* excretory (renal) system, the excretory duct cell and pore cell. Lipocalins are a large family of secreted proteins that transport lipophilic cargos and participate in intercellular signaling. *lpr-1* is required at a time of rapid luminal growth, it is expressed by the duct, pore and surrounding cells, and it can function cell nonautonomously. These results reveal a novel signaling mechanism that controls unicellular tube formation, and provide a genetic model system for dissecting lipocalin signaling pathways.

Keywords

Lipocalin; Tubulogenesis; Intercellular signaling; *lpr-1*; Excretory

Introduction

Tubes are an essential component of many organs such as the kidney, lungs, and vasculature (Lubarsky and Krasnow, 2003). These tubes can vary widely in size and structure, but all have an apical surface lining a hollow lumen through which vital liquids or gases can be transported. Although tubes can be many cells in diameter, the smallest tubes are unicellular. Examples of such unicellular tubes include many capillaries found in the terminal vascular bed of mammalian organs such as the kidney, duodenumand cerebral cortex (Bar et al., 1984), specialized tip cells in the trachea of *Drosophila* (Samakovlis et al., 1996), and a variety of epithelial, glial and mesodermal cells in the nematode *C. elegans* (Buechner et al., 1999; Nelson et al., 1983; Perens and Shaham, 2005; Rasmussen et al., 2008; Ward et al., 1975).

Unicellular tubes can form by either wrapping or hollowing mechanisms. During wrapping, the cell body folds around and forms an adherens junction with itself (termed an autocellular junction), and the resulting lumen is formed from a previously extracellular space

*Corresponding author. sundaram@mail.med.upenn.edu (M.V. Sundaram).

(Rasmussen et al., 2008; Ribeiro et al., 2004). In contrast, during hollowing, vesicular structures within a cell's cytoplasm coalesce and grow to form an eventual interior lumen (Berry et al., 2003; Buechner, 2002; Davis and Camarillo, 1996; Folkman and Haudenschild, 1980; Kamei et al., 2006). Such tubes are termed “seamless” because they lack autocellular junctions (Bar et al., 1984). Recently, it has been shown that cells that form unicellular tubes by wrapping also can lose their autocellular junctions and become seamless through a self-fusion event (Rasmussen et al., 2008). Whether formed initially by wrapping or hollowing, the lumen of a unicellular tube often grows extensively during development and must connect with that of other tubes to generate a functional conduit. The molecular signals that control lumen formation, growth, and connectivity are poorly understood.

The *C. elegans* excretory (renal) system is a simple model system for studying unicellular tube formation, since it consists of only three connected unicellular tubes (Nelson et al., 1983) (Fig. 1). Two of these tubes (the excretory canal cell and duct cell) are seamless; the canal cell forms a tube by a hollowing mechanism (Berry et al., 2003; Buechner, 2002), while the duct cell appears to form a tube through wrapping and self-fusion (see Results). The third tube (the pore) has an autocellular junction and thus forms by wrapping. The largest of these tube cells is the excretory canal cell, whose cell body is located in the head of the animal, but which extends two hollowtubules, termed canals, anteriorly and posteriorly along the entire length of the animal, forming a large H-shape (Buechner, 2002). The canal cell has an apical cytoskeleton that stabilizes the luminal structure and maintains its uniform size and shape (Buechner, 2002; Gobel et al., 2004). The canals, which are closed at their termini, collect and transport fluid to the excretory cell body for subsequent expulsion through the duct and pore cells (Nelson et al., 1983; Nelson and Riddle, 1984). The canals join at the excretory sinus within the excretory canal cell body, and the sinus forms an apical junction (termed the “secretory junction”) to connect with the excretory duct cell (Nelson et al., 1983). The duct cell connects to the pore cell through another apical junction, and together the duct and pore lumina (which are both lined with cuticle, unlike the canal cell lumen) form a continuous channel that opens out of the body, allowing fluid to be excreted (Nelson et al., 1983; Nelson and Riddle, 1984).

The excretory system functions as the primitive renal system of the worm and has an essential role in osmoregulation. Larvae in which any of the three tubular cells are ablated accumulate fluid within the body cavity and die with a characteristic rod-like morphology (Nelson and Riddle, 1984). Mutants that lack the excretory duct cell (Yochem et al., 1997) or mutants that have physiological defects in excretory system function (Liegeois et al., 2007), have a similar rod-like lethal phenotype, arresting at an early larval stage. This distinctive phenotype can be used to identify gene products important for various steps of excretory system development or function.

Here we describe several interesting aspects of excretory duct and pore development and identify *lpr-1* as a gene important for connection between these two unicellular tubes.

Results

Timeline of duct and pore development in wild-type

We first examined the time course of duct and pore cell development in wild-type animals (summarized in Fig. 1). The presumptive duct and pore cells are born on the left and right sides, respectively, of the developing embryo, and then migrate towards the ventral midline during enclosure (Sulston et al., 1983). The fates of these cells are specified by Ras-mediated signaling, which promotes the duct (vs. pore or “G1”) fate (Yochem et al., 1997). The cells adopt stereotypic positions adjacent to the excretory canal cell by the comma stage of embryogenesis, at which time the secretory junction between the canal cell and duct cell

becomes detectable with the adherens junction marker AJM-1::GFP (data not shown). By the 3-fold stage of embryogenesis, AJM-1::GFP also marks the junctions between the duct cell and pore cell, between the pore cell and ventral epithelium, and the pore cell autocellular junction (Figs. 1–3). In wild-type embryos and larvae, the duct cell lacks a visible autocellular junction, but in larvae mutant for the fusogen *aff-1* (Sapir et al., 2007), the duct now has an autocellular junction (Fig. 2), suggesting that the duct cell forms a seamless tube through a wrapping and self-fusion mechanism (Rasmussen et al., 2008).

TEM analysis of archival wild-type embryos revealed that the duct is seamless and lumen is continuous through the canal, duct and pore cells by the 1.5-fold stage (Fig. 1A). The duct cell initially has a compact, block-like shape and a simple, linear lumen, but as the worm elongates and grows to the 3-fold stage, the duct cell changes shape and stretches, while the duct lumen expands greatly in length, looping through the cell body and then within a narrow cell process to connect to the pore cell (Fig. 1B). Thus, wrapping of the duct and pore cells and the initial connection of their lumina must occur at or soon after the comma stage, with significant duct luminal growth and cellular morphogenesis continuing into the 3-fold stage.

After hatching, pore identity changes and the duct–pore connection must be remodeled (Sulston and Horvitz, 1977; Sulston et al., 1983). During the latter part of the first larval stage, the embryonic excretory pore cell (G1) withdraws from the excretory system and divides to generate two neuronal daughters. As G1 withdraws, a neighboring cell, G2, takes over pore function, apparently first wrapping around the ventral portion of the pore opening (Fig. 1C). Later in the second larval stage, G2 divides and its daughter G2.p becomes the pore. These are interesting cases of epithelial remodeling and apparent transdifferentiation.

lpr-1 mutants arrest with severely distorted excretory canals

To identify genes important for excretory tube development, we performed an EMS mutagenesis screen for rod-like lethal mutants. One of the mutants we identified is *lpr-1(cs73)*. A second, cold-sensitive allele of *lpr-1*, *h276* (originally called *let-124*), was kindly provided by Ann Rose (U. of British Columbia). *lpr-1* mutants have a recessive, incompletely penetrant zygotic lethal phenotype, with >90% of the mutants dying during or before the first larval stage (Table 1). These larvae have severely truncated and abnormal excretory canals, as visualized with the canal cell marker *vha-1::GFP* (Figs. 3B, D). The remaining mutants survive to become fertile adults, and appear essentially normal, with only mild shortening of the excretory canals (data not shown). Therefore, the mutant strains can be propagated as homozygous stocks (Table 1). Based on genetic studies with the deficiency *hDf10*, *cs73* appears to be a strong loss-of-function allele, while *h276* is hypomorphic (Table 1).

lpr-1 encodes a lipocalin-related protein

We mapped *cs73* to the left arm of chromosome I by standard methods and obtained rescue of *cs73* rod-like lethality with fosmids WRM0630CF11 andWRM0611DH06 (Geneservice, UK) (Materials and methods). Three candidate genes were covered by both fosmids. We amplified their genomic sequences from *cs73* mutants and sequenced their predicted coding regions and splice junctions. Only Y65B4BR.2 contained a molecular lesion (Fig. 4B). We rescued *cs73* rod-like lethality with a 7.7 kb XhoI/HindIII genomic fragment (pCS1) containing only the Y65B4BR.2 gene, as well as with a Y65B4BR.2 cDNA construct (Table 1, Figs. 4A, B). We conclude that *lpr-1* is Y65B4BR.2.

We characterized three Y65B4BR.2 cDNA clones as well as RT-PCR products and found evidence for three splice isoforms, but only one (isoform a) appeared functional in

transgenic rescue assays (Fig. 4B and Materials and methods). *lpr-1(cs73)* mutants have a G to A nucleotide change that affects a splice donor site in isoform a (Fig. 4B). RT-PCR analysis showed that *cs73* can eliminate splicing, leading to an in-frame insertion, or can result in use of a cryptic splice donor site, leading to an in-frame deletion (Fig. 4C). Although *cs73* is not a molecular null, our genetic analysis (Table 1) indicates that it is a strong loss-of-function allele.

lpr-1(*h276*) mapped to the same region and failed to complement *cs73*, and its lethality could also be rescued with the Y65B4BR.2 genomic rescue construct (Table 1 and data not shown). Nevertheless, we did not find a molecular lesion in *h276* mutants within the Y65B4BR.2 coding region, the exon/intron boundaries, nor the 5′ or 3′ flanking regions present within the Y65B4BR.2 genomic fragment. Y65B4BR.2 introns are highly repetitive, and we could not fully sequence them, leaving open the possibility that a lesion is present in one of these introns. By real-time PCR, we found that Y65B4BR.2 RNA transcript levels are reduced 5-fold in *h276* mutant embryos compared to wild-type (Fig. 5). The *h276* allele may therefore contain a molecular lesion in an unidentified regulatory element.

Conceptual translation of Y65B4BR.2a predicts a protein of the Lipocalin family (Fig. 4D). Lipocalins are small, secreted proteins that are generally believed to deliver small lipophilic cargos to target cells via interactions with specific, membrane-bound receptors (Blaner, 2007;Devireddy et al., 2005;Flower, 2000). Lipocalins share a common tertiary structure but have little overall sequence homology beyond a short lipocalin signature sequence (Flower et al., 2000). They have an eight-stranded anti-parallel beta barrel that forms a “cup-like” structure for cargo binding, and this barrel is flanked by N-and C-terminal helices (Flower et al., 1993;Ganfornina et al., 2000). Y65B4BR.2a has all of the expected features of a lipocalin, including: 1) a predicted signal sequence for secretion at its N-terminus according to SMART protein database (Schultz et al., 1998), 2) an internal lipocalin signature sequence matching the consensus [DENG]-{A}-[DENQGSTARK]-×(0,2)-[DENQARK]-[LIVFY]-{CP}-G-{C}-W-[FYWLRH]-{D}-[LIVMTA] (Prosite pattern PS00213) (Hulo et al., 2008), and 3) a predicted eight-stranded beta barrel flanked by N- and C-terminal helices according to the SCOP (Structural Classification of Proteins) and PredictProtein databases (Andreeva et al., 2008;Rost et al., 2004).We therefore named Y65B4BR.2 *lpr-1* (*Li*P*ocalin* *R*elated-1).

Structural prediction databases (Andreeva et al., 2008) identify only six lipocalins in the *C. elegans* genome, much fewer than the >50 predicted in mammalian genomes. The lack of sequence conservation among lipocalins makes it difficult to identify a specific ortholog of LPR-1 outside of nematodes, or to predict its likely cargo. Nevertheless, the finding that *lpr-1* encodes a lipocalin suggests that a novel lipocalin-based signaling mechanism controls some aspect of excretory system development or function.

lpr-1 mutants lack a continuous lumen between the duct and pore cells

The rod-like lethality and excretory canal abnormalities observed in *lpr-1* mutants potentially could be explained by defects in cell fate specification, tubular morphogenesis, or subsequent osmoregulation. Marker analysis suggested that all relevant excretory system cell types were present, including the excretory canal cell, duct cell, pore cell, and canal-associated neurons (Figs. 3B, D, F, H, Table 2), arguing against a role for *lpr-1* in cell type specification. Temporal rescue experiments (see below) and observations of developing *lpr-1* embryos instead pointed to a morphogenetic role in joining the unicellular tubes to form a functional conduit.

In *lpr-1* embryos, the excretory canal cell body and its developing canals appear normal up until the late 3-fold stage of embryogenesis, around the time that the excretory system may

begin functioning (Nelson and Riddle, 1984). By 1.5 h before hatch, in >90% of *lpr-1* embryos (n = 29), a swelling develops within the excretory canal cell body (Fig. 3F). Additional swellings appear within the canals shortly thereafter, suggesting that fluid accumulates initially within the excretory sinus and then spreads posteriorly within the canal lumina. As the swellings increase in size, the excretory canals retract into a bolus comprised of multiple, hollow, circular structures or "cysts" (Fig. 3D). This bolus eventually bursts and fluid rapidly accumulates throughout the body cavity, apparently leading to the rod-like lethal phenotype. Since the first excretory canal cell swellings appear near the junction with the duct, it appears that fluid is unable to be passed out of the excretory canal cell and through the duct and pore cells.

To observe duct cell and pore cell morphology more closely, we made use of the adherens junction marker AJM-1::GFP (Koppen et al., 2001). In wild-type embryos at the late 3-fold stage, AJM-1::GFP marks the secretory junction between the excretory canal cell and duct cell, and junctions between the duct cell and pore cell, between the pore cell and ventral epithelium, and the pore cell autocellular junction (Figs. 1B, 2A, 3E). In *lpr-1* mutants, all of these junctions appear intact, yet fluid accumulates immediately posterior to the secretory junction (Fig. 3F, Table 2). Additional studies with the predominantly cytoplasmic marker HMP-1::GFP confirmed that the canal cell, duct cell and pore cell bodies are normally positioned and in close contact (Figs. 3G, H, Table 2). Together with the ultrastructural data below, these data suggest that pore cell wrapping does occur and that all three tube cells form apical junctions to connect to each other appropriately, but that the lumina are not fully connected.

We observed excretory system lumen structure in *lpr-1* mutants by performing transmission electron microscopy (TEM) of serial thin sections (summarized in Fig. 6A). Late three-fold stage embryos were selected for this analysis, since that is the stage when *lpr-1* mutant defects first become apparent by light microscopy. In normal late 3-fold embryos, TEM reveals a continuous lumen through the excretory canal cell, duct and pore (Fig. 1B). In *lpr-1* 3-fold embryos, the excretory canal cell lumen is widened but otherwise appears normal and connects with the duct lumen through the secretory junction in 4/4 animals examined (Fig. 6G). The duct lumen is continuous up to within 300–600 nm of the duct–pore cellular junction. However, in 4/4 embryos, the duct lumen terminates prematurely within the duct cell (Figs. 6C–E), and does not connect to the pore lumen (Fig. 6B). The pore cell itself, however, appears normal and opens to the outside environment (Fig. 6F). In the distal region of the duct cell near the point where the lumen terminates, multiple disconnected vesicles are often present, and some of these vesicles appear to span the duct–pore cellular junction (Fig. 6B). *lpr-1* is therefore required to connect or stabilize the duct and pore lumina at the site where they meet.

Since the excretory canal cell lumen appears continuous at this embryonic stage, the canal cell defects observed in *lpr-1* mutant larvae could be a secondary consequence of fluid backup. The partially lumen-less duct cell probably acts as a "stopper" by blocking fluid movement from the canal cell to the pore cell. The remaining duct cell lumen has a cuticle lining which may stabilize it to prevent swelling, whereas the excretory canal cell lumen, which lacks cuticle, may be more prone to distortion as fluid accumulates. We cannot exclude the possibility that LPR-1 directly impacts the canal cell lumen. However, since the earliest defect in *lpr-1* embryos is in the connection between the duct and pore lumina, we propose that one or both of these cells are the primary target of LPR-1 action.

lpr-1 is required at the time that significant duct lumen growth occurs

To determine when during duct and pore development *lpr-1* is required, we expressed a heat-shock inducible *hsp16.2::lpr-1(+)* transgene in *lpr-1(cs73)* animals at various time

points throughout embryogenesis as well as during the first larval stage (Fig. 7). A pulse of *lpr-1(+)* expression at the comma stage completely rescued *lpr-1(cs73)* lethality and excretory canal defects. Rescue decreased somewhat when *lpr-1(+)* was expressed at the two-fold stage, and decreased dramatically at the early three-fold stage. We observed no rescue when *lpr-1(+)* was expressed during the first larval stage. These experiments confirm that *lpr-1* acts after the time of cell fate specification and is not required continuously for osmoregulation or the maintenance of luminal integrity. Furthermore, *lpr-1* appears to act after the time of initial duct and pore tubulogenesis, and well before the time of G1-to-G2 pore swapping. Instead, *lpr-1* is required during the discrete interval when significant duct lumen outgrowth occurs (see Fig. 1D). This temporal requirement is consistent with our phenotypic analysis above, and suggests that *lpr-1* may not be required for the initial connectivity of the lumina, but rather for the maintenance of this connection during cellular and luminal growth (see Discussion).

lpr-1 is expressed in the excretory duct, excretory pore and surrounding epidermal cells

To determine in what cells *lpr-1* is transcribed, we generated an *lpr-1*::GFP transcriptional reporter in which the GFP coding region (with stop codon) was inserted at the LPR-1 ATG within the complete *lpr-1* genomic rescue fragment (Fig. 8A). This strategy preserves all potential *lpr-1* regulatory elements. Consistent *lpr-1*::GFP expression initiates immediately after the comma stage of embryogenesis and continues throughout the remainder of embryonic and larval development. At the three-fold stage of embryogenesis, *lpr-1*::GFP is expressed within both the excretory duct cell and pore cell, and in G2, which adopts excretory pore cell function later in development (Sulston et al., 1983) (Figs. 8D, E). We observed no expression within the excretory canal cell. *lpr-1*::GFP is also expressed in hyp7, seam cells, and P cells (Figs. 8B, C), all of which are epidermal cell types that surround the excretory system. Thus *lpr-1* is expressed by a variety of cell types surrounding the excretory system, as well as by the duct and pore cells themselves. If LPR-1 protein is expressed in all of these cells and is secreted as predicted, the protein could be present at either the basal or apical (luminal) surfaces of the duct cell and pore cell.

lpr-1 functions cell non-autonomously

Since LPR-1 is predicted to be a secreted protein, we tested if it could function cell non-autonomously. To test if *lpr-1* expression outside of the duct cell is sufficient for it to act in excretory system morphogenesis, we used a 216 bp fragment of the epidermal specific promoter *dpy-7* to drive *lpr-1* expression in *lpr-1(cs73)* mutants (Gilleard et al., 1997; Myers and Greenwald, 2005). In embryos, we found that this promoter drives detectable expression in hyp7, seam cells, P cells and the pore cell, but not in the duct cell (data not shown). *dpy-7p::LPR-1* almost completely rescued *lpr-1(cs73)* rod-like lethality (Fig. 8F) as well as excretory canal morphology (data not shown), suggesting that epidermal and/or excretory pore expression of LPR-1 is sufficient for function.

Next, we addressed if *lpr-1* could act in excretory system morphogenesis even when it is made within a tissue where we never observe its expression. We expressed *lpr-1* in body wall muscle under control of the *unc-54* promoter (Graham et al., 1997; Okkema et al., 1993). We confirmed that, in embryos, this promoter drives detectable expression only in body muscle, and not in any cells of the excretory system. Similar to *dpy-7p::LPR-1*, the *unc-54p::LPR-1* transgene rescued *lpr-1(cs73)* mutant rod-like lethality (Fig. 8F) and excretory canal morphology (data not shown). Taken together, the *dpy-7p::LPR-1* and *unc-54p::LPR-1* rescue data show that *lpr-1* does not need to be made in a specific place, and support a model in which secreted LPR-1 acts cell non-autonomously to promote duct–pore lumen connectivity.

Discussion

In mammals, unicellular tubes appear to be prevalent in the microvasculature, the capillary beds that feed organs such as the brain and kidney (Bar et al., 1984). When human vascular endothelial cells are cultured *in vitro*, or when zebrafish vascular endothelial cells are observed *in vivo*, they initially form unicellular tubes before assembling into more complex multicellular tubules, suggesting that unicellular tubes could be developmental intermediates in the formation of other tube types (Blum et al., 2008; Folkman and Haudenschild, 1980; Kamei et al., 2006). Defects in the formation or maintenance of unicellular tubes would be expected to have severe consequences for human health, including kidney disease and stroke (Nangaku and Fujita, 2008;Wang and Shuaib, 2007; Whitehead et al., 2009), yet little is known about how unicellular tubes form lumen and connect with one another. Animal models such as the *C. elegans* system described here will be important in dissecting the molecular mechanisms controlling unicellular tube formation and connectivity.

Our studies demonstrate that a lipocalin functions cell non-autonomously to control luminal connectivity between two unicellular tubes in the *C. elegans* excretory system. Lipocalins are a large family of proteins and have been implicated in a variety of intercellular signaling events, including those controlling kidney tubulogenesis or repair (Schmidt-Ott et al., 2007; Yang et al., 2003). Nevertheless, only a few genetic models for lipocalin function exist (Flo et al., 2004; Quadro et al., 1999; Sanchez et al., 2006). Thus, our studies not only implicate a novel signaling mechanism in the control of unicellular tube development, but also provide a powerful genetic system for further dissection of lipocalin signaling pathways.

Formation of seamless tubes by wrapping and self-fusion

The excretory duct cell appears to form a seamless tube through a wrapping and self-fusion mechanism similar to that recently described for two cells at the interface of the *C. elegans* pharynx and intestine (Rasmussen et al., 2008). Self-fusion requires AFF-1, one of two transmembrane proteins known to act as homotypic cellular fusogens in a variety of *C. elegans* cell types (Sapir et al., 2007). Self-fusion is not absolutely essential for duct cell function, but may help prevent fluid leakage, as a small percentage of *aff-1* mutants accumulate fluid in their body cavities and die as rod-like larvae (Sapir et al., 2007 and data not shown). Although seamless tubes traditionally have been thought to form by hollowing (Lubarsky and Krasnow, 2003), the prevalence of self-fusion in *C. elegans* seamless tubes raises the possibility that many seamless tubes in other organisms may also form by wrapping and self-fusion.

LPR-1 signaling promotes luminal connectivity

Once formed, the duct cell lumen must connect to the lumina of the canal cell and the pore cell and then grow extensively in length while maintaining these connections. This addition of duct lumen likely requires rapid synthesis of apical membrane components, and vesicular trafficking and fusion to deliver these components to the pre-existing main lumen.

We have shown that the lipocalin LPR-1 is required for connectivity of the duct and pore lumina. In *lpr-1* mutants at the 3-fold stage, the duct lumen terminates prematurely within the duct cell body, giving way to disconnected vesicles. At this point we do not know if the duct and pore lumina never connect in these mutants, or if the lumina connect but then break during subsequent development — alternatives that can only be resolved definitively through further TEM studies. These two alternatives have rather different implications. If *lpr-1* is required for the initial connection, this implies a role in coordinating the duct and pore cells as they curl up to form tubes, and somehow preventing their new lumina from closing off at their intercellular junction. On the other hand, if *lpr-1* is required to maintain

the luminal connection during development, it may play a role in strengthening or building more lumen as the cells elongate. Our temporal rescue experiments (Fig. 7) seem more consistent with the latter possibility. If lumen breakage does occur in *lpr-1* mutants, it may be caused by a failure of the duct lumen to grow at a sufficient pace during duct process elongation, or may reflect a more specific structural defect at the duct–pore interface. Notably, discontinuous lumina were observed only in the most anterior region of the duct cell near its junction with the pore cell, suggesting a special character of the lumen in that region.

We have also shown that *lpr-1* functions cell non-autonomously, suggesting a signaling function. *lpr-1* is broadly expressed in epithelial cells and in the duct and pore cells themselves, and the protein is likely secreted from these cells to bathe the region of the duct–pore cell junction. Since ectopic basal expression is sufficient for *lpr-1* rescue (without obvious deleterious effects), the precise source of LPR-1 does not seem to be important and is unlikely to convey positional information about where lumen connections or outgrowth should occur. Instead, LPR-1 may play a permissive role in connectivity or growth. By analogy to other characterized lipocalins (see below), LPR-1 may sequester some cargo, deliver a cargo for uptake into cells and/or stimulate a signal transduction cascade. The duct, pore, or both cells may be relevant LPR-1 targets.

Interestingly, studies of two other unicellular tubes in *C. elegans*, the amphid sheath and socket glia, have also implicated intercellular signaling in lumen formation and connectivity. The Patched-related transmembrane protein DAF-6 and an unknown cue derived from the amphid sensory neurons are required for connectivity of the sheath and socket lumina, and have been proposed to regulate the balance between exocytic and endocytic vesicle trafficking (Perens and Shaham, 2005). Although DAF-6 and LPR-1 are individually required for connectivity of distinct lumina, there are indications that both play wider roles in lumen formation. DAF-6 lines most tubular lumina and acts redundantly with the Dispatched-related transmembrane protein CHE-14 to affect their development (Michaux et al., 2000; Perens and Shaham, 2005). LPR-1 is also widely expressed, and *lpr-1* mutant escapers that survive past the L1 stage have shortened excretory canals (data not shown) and defects in either the phasmid sensory neurons or their glia (Table 3). While their distinct tissue-specificities make it unlikely that LPR-1 signals through DAF-6, LPR-1 could potentially act through another DAF-6-related transmembrane protein to control vesicular trafficking and lumen growth.

Another possibility is that LPR-1 delivers directly or promotes the synthesis of apical membrane components that make up the newly added duct lumen. Consistent with such a model, the *lpr-1* vesicle accumulation phenotype has some similarity to that of mutants for the ELAV splicing factor homolog EXC-7, which has been proposed to regulate expression of SMA-1/B-spectrin and other apical membrane proteins and is required for complete outgrowth of the excretory canal lumina (Fujita et al., 2003). *lpr-1* mutants could have similar deficits in structural components of the duct lumen that hinder outgrowth or stability.

A genetic system for dissecting lipocalin signaling

LPR-1 is the first of at least six *C. elegans* lipocalins to be characterized. There are >50 predicted lipocalins in mammals (SCOP database), and studies of a small subset suggest that lipocalins bind small, lipophilic molecules such as sterols, odorants or heme groups, and deliver these cargos to target cells via interactions with specific transmembrane receptors (Flower et al., 2000; Quadro et al.,1999). An archetypal lipocalin is mammalian Retinol Binding Protein (RBP), which delivers retinol to target tissues via interaction with a recently identified RBP receptor, STRA6 (Kawaguchi et al., 2007; Redondo et al., 2006). The internalized retinol can then be converted to retinoic acid and act in nuclear hormone

receptor signaling (Flower, 2000; Goodman, 2006). Another highly studied lipocalin is Neutrophil Gelatinase Associated Lipocalin (NGAL), which binds to an iron-chelating siderophore and delivers iron to target tissues via interaction with a distinct NGAL receptor (Devireddy et al., 2005; Yang et al., 2002). Some lipocalins, including NGAL, may also act by sequestering their cargos (Flo et al., 2004) or may act independently of cargo to stimulate receptor-mediated signaling pathways (Chamero et al., 2007; Gwira et al., 2005). The cargoes, receptors, downstream signaling pathways and biological functions of most mammalian lipocalins are unknown. With the powerful genetic approaches available in *C. elegans*, studies of LPR-1 and the other *C. elegans* lipocalins are likely to provide important insights into the regulation and function of this poorly understood protein family.

Interestingly, NGAL (also known as 24p3 or lipocalin-2) has been implicated in the development of multicellular tubes in the kidney (Schmidt-Ott et al., 2007). NGAL is secreted from the ureteric bud and can induce metanephric mesenchyme to express epithelial markers and form tubular nephrons in culture (Yang et al., 2002). In mouse kidney mIMCD-3 cells, NGAL knockdown interferes with hepatocyte growth factor (HGF)-stimulated tubulogenesis, resulting in multicellular cyst formation (Gwira et al., 2005). In humans, NGAL expression is rapidly induced in response to kidney injury or stress, and is used by physicians as a biomarker to monitor patient status (Mishra et al., 2005; Mishra et al., 2003; Schmidt-Ott et al., 2006). While these studies suggest a potential role for NGAL in kidney nephron tubulogenesis, mouse knockouts of NGAL/lipocalin-2 display no obvious kidney defects, perhaps due to genetic redundancy (Berger et al., 2006; Flo et al., 2004). It will be interesting to determine whether NGAL and LPR-1 promote tubulogenesis through related or distinct mechanisms.

To our knowledge, *C. elegans lpr-1* provides the first genetically tractable model system for dissecting the molecular pathways through which a lipocalin can control tubulogenesis. We are characterizing other mutants with an *lpr-1*-like mutant phenotype as well as a set of *lpr-1* suppressors that should give further insight into how LPR-1 controls lumen connectivity.

Materials and methods

Strains and phenotypic analysis

Strains were maintained and manipulated by standard methods unless otherwise noted. Bristol N2 was the wild-type strain. *lpr-1 (cs73)* was isolated after EMS mutagenesis of the N2 strain, and was outcrossed twice before phenotypic analysis. Linkage mapping placed *lpr-1* very close to *bli-3* and to the left of SNP pKP1100. All mapping data are available at Wormbase (www.wormbase.org).

To quantify the degree of *lpr-1* lethality, hermaphrodites were allowed to lay eggs on NGM plates for 6– 10 h. Percent lethality was determined by the proportion of progeny that failed to reach the L4 larval stage 48 h post-egg lay. To assess whether all relevant cell types were present and properly positioned (Table 2),we used the following markers: *vha-1*::GFP (Oka et al., 1997) (excretory canal cell), *lin-48*:: GFP (Johnson et al., 2001) (duct cell), *lpr-1*::GFP (this work), AJM-1:: GFP (Koppen et al., 2001) and HMP-1::GFP (J. Hardin, personal communication (duct and pore cells), *ceh-23*::GFP (Forrester et al., 1998) (canal-associated neurons). Three-fold embryos were paralyzed by treating their mothers with RNAi against the muscle gene *unc-27* to facilitate analyses of marker expression (Kamath et al., 2003).

Quantitative RT-PCR

RNA was extracted from mixed-stage embryos with Trizol (Invitrogen (Carlsbad, CA)), and cDNA was subsequently generated with the Superscript First-Strand Synthesis kit (Invitrogen). RT-PCR was performed with 25 ng cDNA per reaction in triplicate wells. *lpr-1*

TaqMan primers (Applied Biosystems (Foster City, CA)) spanning the exon1/exon2 boundary were used to determine *lpr-1* levels. *smr-1* was used as an endogenous control for normalization. RT-PCR was performed on a 7900HT Fast Real-Time PCR System machine (Applied Biosystems) and all data were analyzed by the comparative C_T method with SDS 2.2.1 software.

Transgenic lines

Details of plasmid generation are available upon request. The *lpr-1* genomic rescue fragment pCS1was cloned from fosmid WRM0630l21. Transgenic lines were generated by co-injection of pCS1 (20 ng/μl) with the marker *unc-119*::GFP (100 ng/μl). The *lpr-1*::GFP transcriptional reporter pCS4 was generated by inserting GFP (with its own stop codon) at the *lpr-1* ATG within the genomic rescue fragment pCS1. Transgenic lines were generated by co-injection of pCS4 (10 ng/μl) with the marker pRF4 (*rol-6sd*) (100 ng/μl) (Mello and Fire, 1995). pCS4 expression was analyzed in a *smg-1(r861)* background to circumvent potential problems with nonsense-mediated decay (Pulak and Anderson, 1993; Wilkinson and Greenwald, 1995).

hsp-16.2::lpr-1a (pCS7), *dpy-7::lpr-1a* (pCS12) and *unc-54::lpr-1a, b,c* (pCS17, pEM1 and pEM2) constructs were generated by inserting the *lpr-1* cDNA into vectors pPD49.78, pKH11 (a derivative of pPD49.26), or pPD30.38, respectively (Addgene). Transgenic lines were generated by co-injecting experimental plasmids at 7 ng/μl and pIM175(*unc-119::gfp*) at 100 ng/μl. *lpr-1(cs73)* mutant lines bearing the *hsp16.2::lpr-1a* transgene were maintained at 15 °C to minimize constitutive expression. We staged animals for our heat-shock experiments by picking comma stage embryos under a dissecting microscope, and incubating them at 15 °C for an empirically determined amount of time [0 h (comma), 2 h (2-fold), 4 h (early 3-fold)] prior to a 1-hour 35 °C heat-shock. L1s were picked and heat-shocked immediately after hatching. We scored for rescue 4 days later by determining the proportion of animals that survived to become L4 larvae to the number of animals that became rod-like lethal larvae. Transgenic L4 larvae and rod-like larvae (vs. non-transgenic siblings) were identified by *unc-119::gfp* expression.

Microscopy

Animals were examined by Nomarski microscopy and epifluorescence using a Zeiss Axioskop (Jena, Germany), and images were taken with a Hamamatsu Chilled CCD Camera (Hamamatsu City, Japan) and analyzed with Adobe Photoshop. Alternatively, animals were examined by confocal microscopy using a Leica TCS SP (Wetzlar, Germany). All confocal images were analyzed with Leica Confocal Software.

For transmission electron microscopy, late 3-fold stage embryos were fixed by high pressure freezing (HPF) followed by freeze substitution (Weimer, 2006), embedded in Eponate resin and cut into serial thin sections between 50 and 100 nm each. Sections of two wild-type and five *lpr-1(cs73)* embryos were observed on a Philips CM10 transmission electron microscope (Amsterdam, The Netherlands) and photographed on Kodak 4489 film or with an Olympus Morada digital camera (Tokyo, Japan). Another similarly prepared and photographed *lin-17* embryo (in which excretory system development appears normal) was kindly provided by Richard Fetter and Cornelia Bargmann (Rockefeller Univ.).

TEM images of young wild-type embryos and of L1 larvae were provided to the Center for *C. elegans* Anatomy by John Sulston and Jonathan Hodgkin (MRC) and by Shai Shaham (Rockefeller Univ.). Embryos EMB1 (1.5-fold), N2 Egg (1.5 fold), Tadpole (comma-1.5 fold) and N2E6B (1.5–2 fold) each reveal a continuous lumen running through the excretory canal cell, duct cell and pore cell (Fig. 1A and data not shown). Larva L1C (mid-L1) shows

the beginning of the G1-to-G2 pore swap (Fig.1C). Many of these images are available at Worm Image (http://www.wormimage.org/).

Acknowledgments

We are indebted to John Sulston, Jonathan Hodgkin, Shai Shaham, Richard Fetter and Cornelia Bargmann for providing archival TEM images of embryos and larvae at various stages of development. These archival images are now stored in the Hall lab. We thank Frank Macaluso, Juan Jimenez and Leslie Gunther for help with high pressure freezing experiments, and especially thank Ken Nguyen, who collected serial thin sections of each new embryo. We thank Emily McMillan for performing functional tests of *lpr-1b* and *lpr-1c*. We thank Christopher Crocker for artwork, Ann Rose, Matthew Buechner, Shai Shaham, Jeff Hardin and the *Caenorhabditis* Genetics Center for providing strains, Yuji Kohara for cDNA clones, and Iva Greenwald, Amin Ghabrial, David Raizen, Todd Lamitina, Mary Mullins, Vincent Mancuso, Kelly Howell and Ishmail Abdus-Saboor for advice and comments on the manuscript. This research was supported by grants from the American Heart Association (0755524U) and NIH (GM058540) to M.V.S. and from NIH (RR12596) to D.H.H. C.E.S. was supported in part by genetics training grant T32GM008216.

References

Andreeva A, Howorth D, Chandonia JM, Brenner SE, Hubbard TJ, Chothia C, Murzin AG. Data growth and its impact on the SCOP database: new developments. Nucleic Acids Res 2008;36:D419–D425. [PubMed: 18000004]

Bar T, Guldner FH, Wolff JR. “Seamless” endothelial cells of blood capillaries. Cell & Tissue Res 1984;235:99–106. [PubMed: 6697387]

Berger T, Togawa A, Duncan GS, Elia AJ, You-Ten A, Wakeham A, Fong HE, Cheung CC, Mak TW. Lipocalin 2-deficient mice exhibit increased sensitivity to *Escherichia coli* infection but not to ischemia-reperfusion injury. Proc. Natl. Acad. Sci. U. S. A 2006;103:1834–1839. [PubMed: 16446425]

Berry KL, Bulow HE, Hall DH, Hobert O. *A C. elegans* CLIC-like protein required for intracellular tube formation and maintenance. Science 2003;302:2134–2137. [PubMed: 14684823]

Blaner WS. STRA6, a cell-surface receptor for retinol-binding protein: the plot thickens. Cell Metabolism 2007;5:164–166. [PubMed: 17339024]

Blum Y, Belting HG, Ellertsdottir E, Herwig L, Luders F, Affolter M. Complex cell rearrangements during intersegmental vessel sprouting and vessel fusion in the zebrafish embryo. Dev. Biol 2008;316:312–322. [PubMed: 18342303]

Buechner M. Tubes and the single *C. elegans* excretory cell. Trends Cell Biol 2002;12:479–484. [PubMed: 12441252]

Buechner M, Hall DH, Bhatt H, Hedgecock EM. Cystic canal mutants in *Caenorhabditis elegans* are defective in the apical membrane domain of the renal (excretory) cell. Dev. Biol 1999;214:227–241. [PubMed: 10491271]

Chamero P, Marton TF, Logan DW, Flanagan K, Cruz JR, Saghatelian A, Cravatt BF, Stowers L. Identification of protein pheromones that promote aggressive behaviour. Nature 2007;450:899–902. [PubMed: 18064011]

Davis GE, Camarillo CW. An alpha 2 beta 1 integrin-dependent pinocytic mechanism involving intracellular vacuole formation and coalescence regulates capillary lumen and tube formation in three-dimensional collagen matrix. Exp. Cell Res 1996;224:39–51. [PubMed: 8612690]

Devireddy LR, Gazin C, Zhu X, Green MR. A cell-surface receptor for lipocalin 24p3 selectively mediates apoptosis and iron uptake. Cell 2005;123:1293–1305. [PubMed: 16377569]

Flo TH, Smith KD, Sato S, Rodriguez DJ, Holmes MA, Strong RK, Akira S, Aderem A. Lipocalin 2 mediates an innate immune response to bacterial infection by sequestrating iron. Nature 2004;432:917–921. [PubMed: 15531878]

Flower DR. Beyond the superfamily: the lipocalin receptors. Biochim. Biophys. Acta 2000;1482:327–336. [PubMed: 11058773]

Flower DR, North AC, Attwood TK. Structure and sequence relationships in the lipocalins and related proteins. Protein Sci 1993;2:753–761. [PubMed: 7684291]

Flower DR, North AC, Sansom CE. The lipocalin protein family: structural and sequence overview. Biochim. Biophys. Acta 2000;1482:9–24. [PubMed: 11058743]

Folkman J, Haudenschild C. Angiogenesis by capillary endothelial cells in culture. Trans. Ophthalmol. Soc. U.K 1980;100:346–353. [PubMed: 6171066]

Forrester WC, Perens E, Zallen JA, Garriga G. Identification of *Caenorhabditis elegans* genes required for neuronal differentiation and migration. Genetics 1998;148:151–165. [PubMed: 9475729]

Fujita M, Hawkinson D, King KV, Hall DH, Sakamoto H, Buechner M. The role of the ELAV homologue EXC-7 in the development of the *Caenorhabditis elegans* excretory canals. Dev. Biol 2003;256:290–301. [PubMed: 12679103]

Ganfornina MD, Gutierrez G, Bastiani M, Sanchez D. A phylogenetic analysis of the lipocalin protein family. Mol. Biol. Evol 2000;17:114–126. [PubMed: 10666711]

Gilleard JS, Barry JD, Johnstone IL. cis regulatory requirements for hypodermal cell-specific expression of the *Caenorhabditis elegans* cuticle collagen *dpy-7*. Mol. Cell Biol 1997;17:2301–2311. [PubMed: 9121480]

Gobel V, Barrett PL, Hall DH, Fleming JT. Lumen morphogenesis in *C. elegans* requires the membrane-cytoskeleton linker *erm-1*. Dev. Cell 2004;6:865–873. [PubMed: 15177034]

Goodman AB. Retinoid receptors, transporters, and metabolizers as therapeutic targets in late onset Alzheimer disease. J. Cell. Physiol 2006;209:598–603. [PubMed: 17001693]

Graham PL, Johnson JJ, Wang S, Sibley MH, Gupta MC, Kramer JM. Type IV collagen is detectable in most, but not all, basement membranes of *Caenorhabditis elegans* and assembles on tissues that do not express it. J. Cell Biol 1997;137:1172–1183.

Gwira JA, Wei F, Ishibe S, Ueland JM, Barasch J, Cantley LG. Expression of neutrophil gelatinase-associated lipocalin regulates epithelial morphogenesis *in vitro*. J. Biol. Chem 2005;280:7875–7882. [PubMed: 15637066]

Hulo N, Bairoch A, Bulliard V, Cerutti L, Cuche BA, de Castro E, Lachaize C, Langendijk-Genevaux PS, Sigrist CJ. The 20 years of PROSITE. Nucleic Acids Res 2008;36:D245–D249. [PubMed: 18003654]

Johnson AD, Fitzsimmons D, Hagman J, Chamberlin HM. EGL-38 Pax regulates the ovo-related gene lin-48 during *Caenorhabditis elegans* organ development. Development 2001;128:2857–2865. [PubMed: 11532910]

Kamath RS, Fraser AG, Dong Y, Poulin G, Durbin R, Gotta M, Kanapin A, Le Bot N, Moreno S, Sohrmann M, Welchman DP, Zipperlen P, Ahringer J. Systematic functional analysis of the *Caenorhabditis elegans* genome using RNAi. Nature 2003;421:231–237. [PubMed: 12529635]

Kamei M, Saunders WB, Bayless KJ, Dye L, Davis GE, Weinstein BM. Endothelial tubes assemble from intracellular vacuoles *in vivo*. Nature 2006;442:453–456. [PubMed: 16799567]

Kawaguchi R, Yu J, Honda J, Hu J, Whitelegge J, Ping P, Wiita P, Bok D, Sun H. A membrane receptor for retinol binding protein mediates cellular uptake of vitamin A. Science 2007;315:820–825. [PubMed: 17255476]

Koppen M, Simske JS, Sims PA, Firestein BL, Hall DH, Radice AD, Rongo C, Hardin JD. Cooperative regulation of AJM-1 controls junctional integrity in *Caenorhabditis elegans* epithelia. Nature Cell Biol 2001;3:983–991. [PubMed: 11715019]

Liegeois S, Benedetto A, Michaux G, Belliard G, Labouesse M. Genes required for osmoregulation and apical secretion in *Caenorhabditis elegans*. Genetics 2007;175:709–724. [PubMed: 17179093]

Lubarsky B, Krasnow MA. Tube morphogenesis: making and shaping biological tubes. Cell 2003;112:19–28. [PubMed: 12526790]

Mello C, Fire A. DNA transformation. Methods Cell Biol 1995;48:451–482. [PubMed: 8531738]

Michaux G, Gansmuller A, Hindelang C, Labouesse M. CHE-14, a protein with a sterol-sensing domain, is required for apical sorting in *C. elegans* ectodermal epithelial cells. Curr. Biol 2000;10:1098–1107. [PubMed: 10996790]

Mishra J, Dent C, Tarabishi R, Mitsnefes MM, Ma Q, Kelly C, Ruff SM, Zahedi K, Shao M, Bean J, Mori K, Barasch J, Devarajan P. Neutrophil gelatinaseassociated lipocalin (NGAL) as a biomarker for acute renal injury after cardiac surgery. Lancet 2005;365:1231–1238. [PubMed: 15811456]

Mishra J, Ma Q, Prada A, Mitsnefes M, Zahedi K, Yang J, Barasch J, Devarajan P. Identification of neutrophil gelatinase-associated lipocalin as a novel early urinary biomarker for ischemic renal injury. J. Am. Soc. Nephrol 2003;14:2534–2543. [PubMed: 14514731]

Myers TR, Greenwald I. lin-35 Rb acts in the major hypodermis to oppose ras-mediated vulval induction in *C. elegans*. Dev. Cell 2005;8:117–123. [PubMed: 15621535]

Nangaku M, Fujita T. Activation of the renin-angiotensin system and chronic hypoxia of the kidney. Hypertens. Res 2008;31:175–184. [PubMed: 18360035]

Nelson FK, Albert PS, Riddle DL. Fine structure of the *C. elegans* secretory-excretory system. J. Ultrastruct. Res 1983;82:156–171. [PubMed: 6827646]

Nelson FK, Riddle DL. Functional study of the *C. elegans* secretory-excretory system using laser microsurgery. J. Exptl. Zool 1984;231:45–56. [PubMed: 6470649]

Oka T, Yamamoto R, Futai M. Three vha genes encode proteolipids of *Caenorhabditis elegans* vacuolar-type ATPase. Gene structures and preferential expression in an H-shaped excretory cell and rectal cells. J. Biol. Chem 1997;272:24387–24392. [PubMed: 9305897]

Okkema PG, Harrison SW, Plunger V, Aryana A, Fire A. Sequence requirements for myosin gene expression and regulation in *Caenorhabditis elegans*. Genetics 1993;135:385–404. [PubMed: 8244003]

Perens EA, Shaham S. *C. elegans daf-6* encodes a patched-related protein required for lumen formation. Dev. Cell 2005;8:893–906. [PubMed: 15935778]

Perkins LA, Hedgecock EM, Thomson JN, Culotti JG. Mutant sensory cilia in the nematode Caenorhabditis elegans. Dev. Biol 1986;117:456–487. [PubMed: 2428682]

Pulak R, Anderson P. mRNA surveillance by the *Caenorhabditis elegans smg* genes. Genes Dev 1993;7:1885–1897. [PubMed: 8104846]

Quadro L, Blaner WS, Salchow DJ, Vogel S, Piantedosi R, Gouras P, Freeman S, Cosma MP, Colantuoni V, Gottesman ME. Impaired retinal function and vitamin A availability in mice lacking retinol-binding protein. EMBO J 1999;18:4633–4644. [PubMed: 10469643]

Rasmussen JP, English K, Tenlen JR, Priess JR. Notch signaling and morphogenesis of single-cell tubes in the *C. elegans* digestive tract. Dev. Cell 2008;14:559–569. [PubMed: 18410731]

Redondo C, Burke BJ, Findlay JB. The retinol-binding protein system: a potential paradigm for steroid-binding globulins? Horm. Metab. Res 2006;38:269–278. [PubMed: 16700009]

Ribeiro C, Neumann M, Affolter M. Genetic control of cell intercalation during tracheal morphogenesis in *Drosophila*. Curr. Biol 2004;14:2197–2207. [PubMed: 15620646]

Rost B, Yachdav G, Liu J. The PredictProtein server. Nucleic Acids Res 2004;32:W321–W326. [PubMed: 15215403]

Samakovlis C, Hacohen N, Manning G, Sutherland DC, Guillemin K, Krasnow MA. Development of the *Drosophila* tracheal system occurs by a series of morphologically distinct but genetically coupled branching events. Development 1996;122:1395–1407. [PubMed: 8625828]

Sanchez D, Lopez-Arias B, Torroja L, Canal I, Wang X, Bastiani MJ, Ganfornina MD. Loss of glial lazarillo, a homolog of apolipoprotein D, reduces lifespan and stress resistance in *Drosophila*. Curr. Biol 2006;16:680–686. [PubMed: 16581513]

Sapir A, Choi J, Leikina E, Avinoam O, Valansi C, Chernomordik LV, Newman AP, Podbilewicz B. AFF-1, a FOS-1-regulated fusogen, mediates fusion of the anchor cell in *C. elegans*. Dev. Cell 2007;12:683–698. [PubMed: 17488621]

Schmidt-Ott KM, Mori K, Kalandadze A, Li JY, Paragas N, Nicholas T, Devarajan P, Barasch J. Neutrophil gelatinase-associated lipocalin-mediated iron traffic in kidney epithelia. Curr. Opin. Nephrol. Hypertens 2006;15:442–449. [PubMed: 16775460]

Schmidt-Ott KM, Mori K, Li JY, Kalandadze A, Cohen DJ, Devarajan P, Barasch J. Dual action of neutrophil gelatinase-associated lipocalin. J. Am. Soc. Nephrol 2007;18:407–413. [PubMed: 17229907]

Schultz J, Milpetz F, Bork P, Ponting CP. SMART, a simple modular architecture research tool: identification of signaling domains. Proc. Natl. Acad. Sci. U. S. A 1998;95:5857–5864. [PubMed: 9600884]

Sulston JE, Horvitz HR. Post-embryonic cell lineages of the nematode *Caenorhabditis elegans*. Dev. Biol 1977;56:110–156. [PubMed: 838129]

Sulston JE, Scheirenberg E, White JG, Thomson JN. The embryonic cell lineage of the nematode *Caenorhabditis elegans*. Dev. Biol 1983;100:64–119. [PubMed: 6684600]

Wang CX, Shuaib A. Critical role of microvasculature basal lamina in ischemic brain injury. Prog. Neurobiol 2007;83:140–148. [PubMed: 17868971]

Ward S, Thomson N, White JG, Brenner S. Electron microscopical reconstruction of the anterior sensory anatomy of the nematode *Caenorhabditis elegans*. J. Comp. Neurol 1975;160:313–337. [PubMed: 1112927]

Weimer RM. Preservation of *C. elegans* tissue via high-pressure freezing and freeze-substitution for ultrastructural analysis and immunocytochemistry. Methods Mol. Biol 2006:203–221. [PubMed: 16988436]

Whitehead KF, Chan AC, Navankasattusas S, Koh W, London NR, Ling J, Mayo AH, Drakos SG, Marchuk DA, Davis GE, Li DY. The cerebral cavernous malformation signaling pathway promotes vascular integrity via Rho GTPases. Nat. Med 2009;15:177–184. [PubMed: 19151728]

Wilkinson HA, Greenwald I. Spatial and temporal patterns of *lin-12* expression during *C. elegans* hermaphrodite development. Genetics 1995;141:513–526. [PubMed: 8647389]

Yang J, Goetz D, Li JY, Wang W, Mori K, Setlik D, Du T, Erdjument-Bromage H, Tempst P, Strong R, Barasch J. An iron delivery pathway mediated by a lipocalin. Mol. Cell 2002;10:1045–1056. [PubMed: 12453413]

Yang J, Mori K, Li JY, Barasch J. Iron, lipocalin, and kidney epithelia. Am. J. Physiol. Renal Physiol 2003;285:F9–F18. [PubMed: 12788784]

Yochem J, Sundaram M, Han M. Ras is required for a limited number of cell fates and not for general proliferation in *Caenorhabditis elegans*. Mol. Cell Biol 1997;17:2716–2722. [PubMed: 9111342]

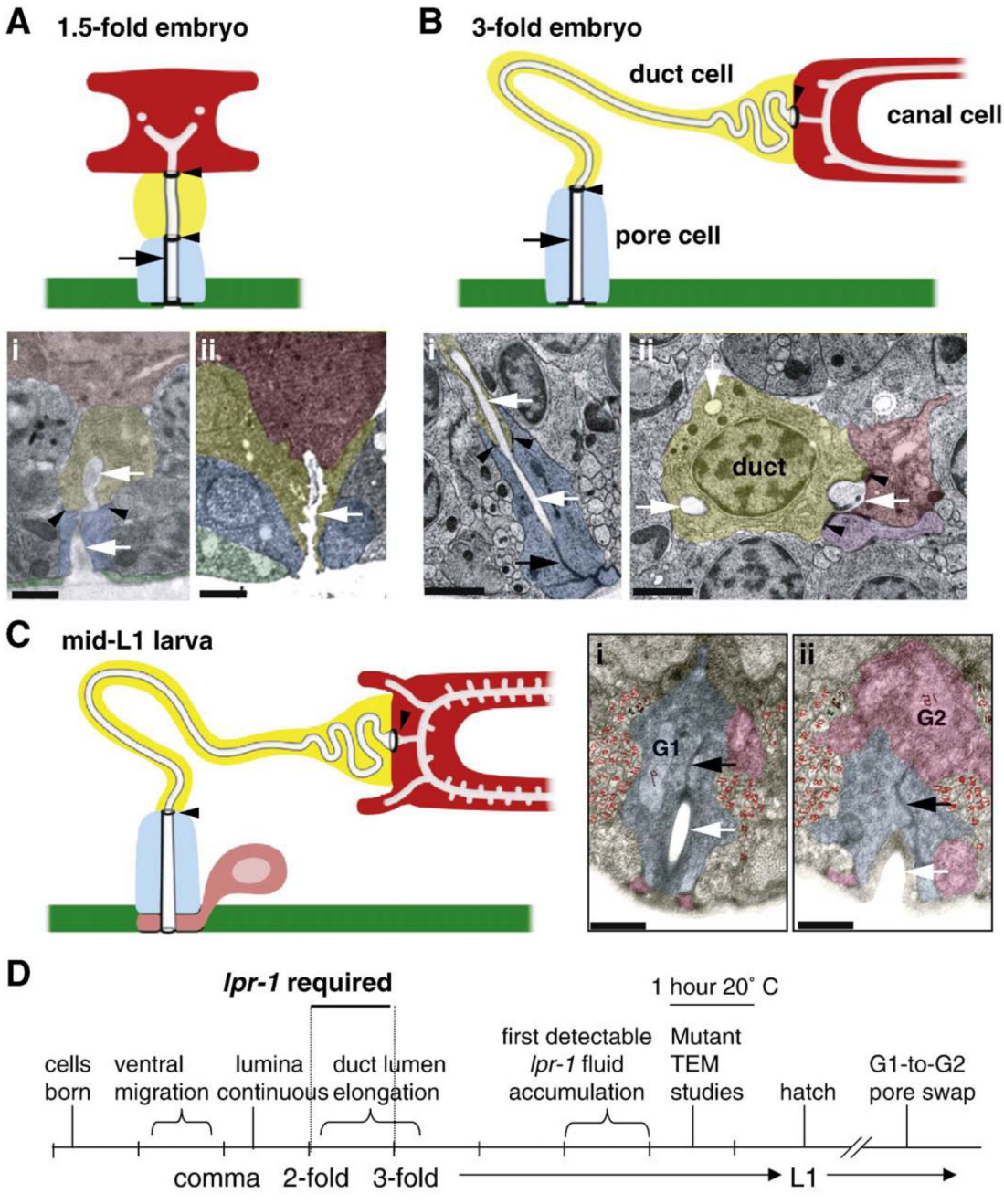

Fig. 1.

Timecourse of excretory system development in wild-type. (A–C) Transmission electron micrographs (TEMs) and corresponding schematics of the excretory system in wild-type animals at different stages. TEMs have been false-colored for clarity. Colored regions represent cell cytoplasm of the canal cell (red), duct cell (yellow), pore cell (blue), or ventral epithelium (green) and uncolored areas represent lumen (indicated by white arrows in TEMs). Thick black circles and lines in schematics indicate *C. elegans* apical junctions, which include the canal/duct and duct/pore intercellular junctions (black arrowheads) and the pore autocellular junction (black arrow). The canal/duct junction has also been termed the “secretory junction” (Nelson et al., 1983). In all images, ventral is on the bottom. In

lateral views, anterior is to left. Scale bars, 1 μm. A) 1.5-fold embryo, anterior view. The cells are compact, and the duct has a short, linear lumen. i) Embryo “N2E6B” TEM kindly provided by Shai Shaham (Rockefeller U.). Anterior view. ii) Embryo “N2 egg” kindly provided by John Sulston (MRC). Lateral view. B) Late 3-fold embryo, lateral view. The tube cells and lumina have expanded in length. For simplicity, only a portion of the canal cell is shown in the schematic. The duct and pore lumina are lined with cuticle (indicated by grey outline), whereas the canal cell lumen is not. i, ii) Two TEM sections from the same embryo, showing i) duct/pore junction, and ii) duct nucleus and cell body (with multiple cross-sections of lumen) and canal/duct junction. These TEM sections are separated by 3–4 μm. Purple color in ii) indicates an excretory gland cell, which also connects to the canal and duct lumina at their junction (Nelson et al., 1983). *lin-17(n677)* embryo kindly provided by Richard Fetter and Cornelia Bargmann (Rockefeller U.). Anterior view. C) Mid-L1 larva, lateral view. i, ii) Adjacent TEM sections show G2 (pink) beginning to take over the ventral-most portion of the pore channel. “L1C” TEMs kindly provided by John Sulston (MRC). Anterior view. D) Timeline of excretory system development, based on (Sulston et al., 1983) and TEM data above.

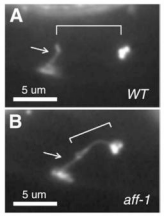

Fig. 2.

The duct tube forms by wrapping and self-fusion. Shown are (A) wild-type and (B) *aff-1(tm2214)* mutant L1 larvae expressing adherens junction marker AJM-1::GFP (Koppen et al., 2001). Arrow indicates pore autocellular junction and bracket indicates the duct cell (which retains an autocellular junction only in *aff-1* mutants).

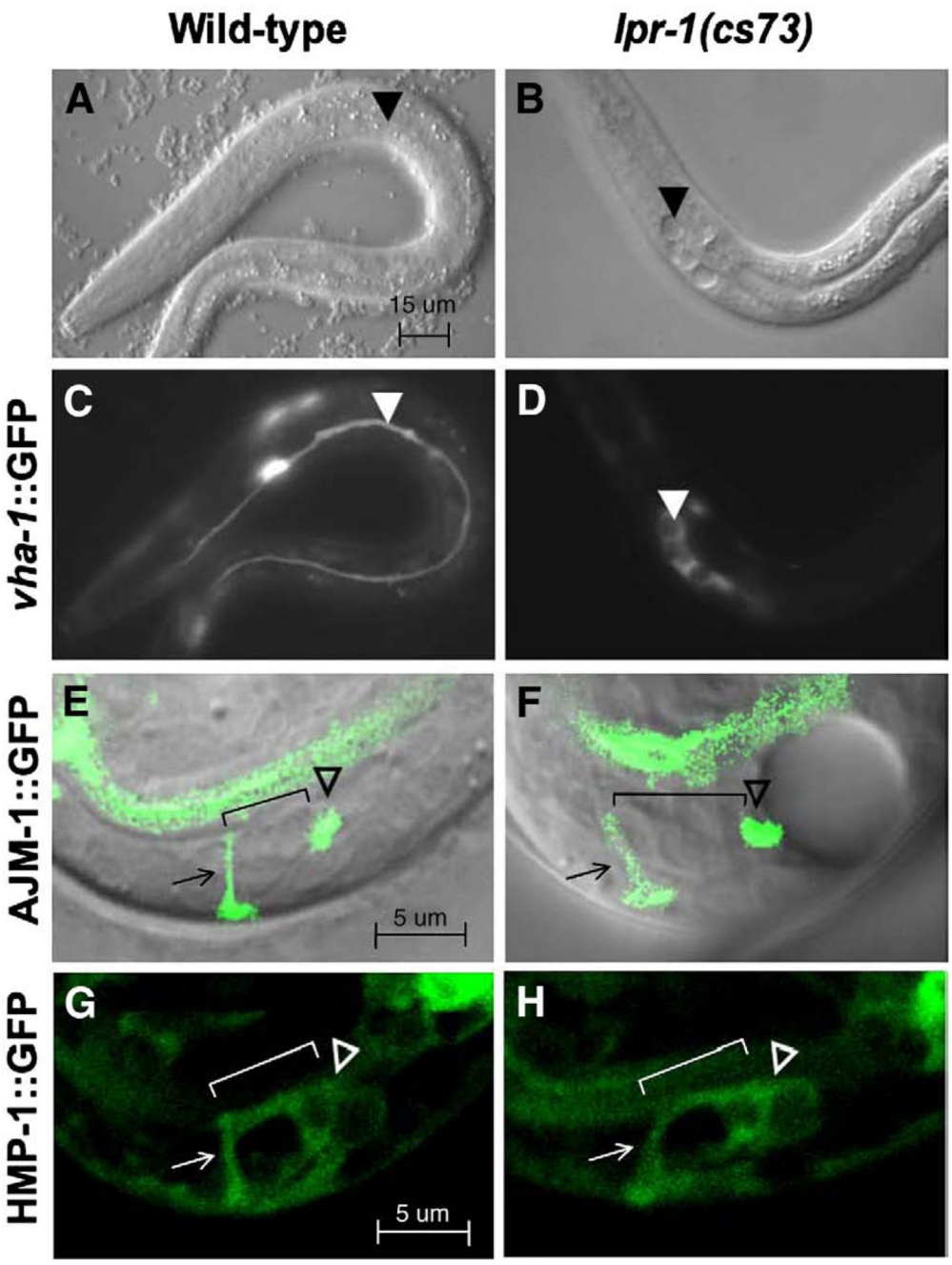

Fig. 3.

lpr-1(cs73) mutants have normally positioned canal, duct and pore cells. In all panels, anterior is to the left and ventral is down. (A, C) Wild-type L1 larva showing excretory canal cell marked with *vha-1*::GFP. (B, D) *lpr-1(cs73)* L1 larva showing severely truncated and cystic excretory canals marked with *vha-1*::GFP. Arrowheads mark canal extensions in A and C, and canal cysts in B and D (E) wild-type and (F) *lpr-1(cs73)* late 3-fold embryos showing apical junctions marked with AJM-1::GFP. Arrow marks the pore cell, hollow arrowhead marks the secretory junction, and bracket indicates position of the duct cell (not visible with AJM-1::GFP). The ring-like structure of the intercellular junctions is not apparent in this lateral view, but could be seen in embryos viewed from the ventral side.

Note the fluid accumulation posterior to the secretory junction in *lpr-1* mutants, causing a dramatic cyst within the excretory canal cell body. (G) wild-type and (H) *lpr-1(cs73)* 3-fold embryos showing canal cell, duct cell and pore cell bodies marked with HMP-1::GFP. Symbols are as above.

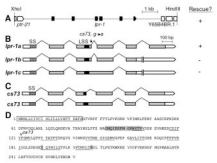

Fig. 4.

lpr-1 encodes a lipocalin. (A) A 7.7 kb XhoI–HindIII genomic fragment (pCS1) containing the Y65B4BR.2 gene rescued *lpr-1* mutant lethality (see Table 1). (B) We found evidence for three *lpr-1* splice variants based on cDNAs ORFeome 3 (isoform a), yk1753f01 (isoform b), and yk817g08 (isoform c) (Genbank FJ174666, FJ174667, and FJ174668, respectively). *lpr-1a* rescued the excretory canal defects and rod-like lethality of *cs73* mutants when expressed under the control of the *hsp16.2*, *dpy-7* or *unc-54* promoters (see Figs. 7, 8F). *lpr-1b* and *lpr-1c* fail to splice out intron 5, leading to a premature stop, and encode truncated proteins that lack a C-terminal alpha helix beyond the predicted beta barrel region. *lpr-1c* also fails to splice out intron 3 and thus inserts an additional 14 amino acids in frame into the beta barrel region. Neither *lpr-1b* nor *lpr-1c* were able to rescue *cs73* lethality when expressed under the control of the *unc-54* promoter: for each construct, four transgenic lines averaged 14% and 12% viability respectively (n> 100 each). *cs73* is a G to A nucleotide transition that affects the intron 3 splice donor site in *lpr-1a* and *lpr-1b*; it would result in a C-to-Y amino acid change in isoform *c*. (C) The consequences of the *cs73* lesion were determined by sequencing the two predominant RT-PCR products obtained from mixed stage mutant worm lysates after amplification with primers flanking intron 3. *cs73* can result in use of a cryptic splice donor 63 nucleotides upstream of the normal intron 3 donor, leading to an in-frame deletion of part of the lipocalin signature sequence (LSS). Alternatively, *cs73* can eliminate intron 3 splicing, leading to an in-frame insertion within the beta barrel region. SS, signal sequence. Grey boxes represent coding exons and white boxes represent untranslated regions. (D) Sequence of the LPR-1A protein. Box indicates signal sequence, shading indicates lipocalin signature sequence and additional amino acids conserved in most lipocalins (Flower et al., 2000) and underlines indicate the eight predicted beta-sheets that make up the lipocalin beta barrel (PredictProtein database, Rost et al., 2004).

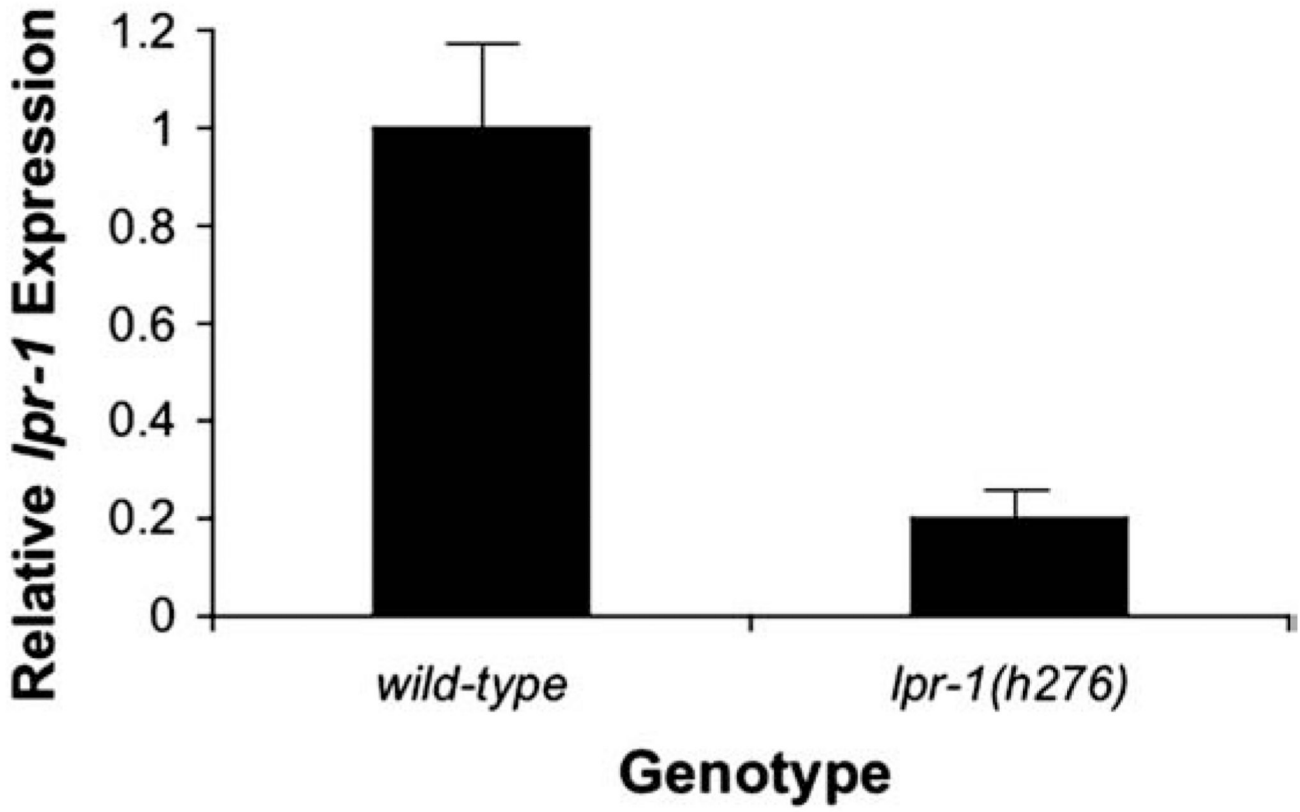

Fig. 5.

lpr-1(h276) has reduced levels of *lpr-1* mRNA. Quantitative Real-Time PCR was performed on either wild-type or *lpr-1(h276)* mixed stage embryos as described in Materials and methods. Black bars indicate relative *lpr-1* mRNA levels with respect to wild-type (which is set to 1).

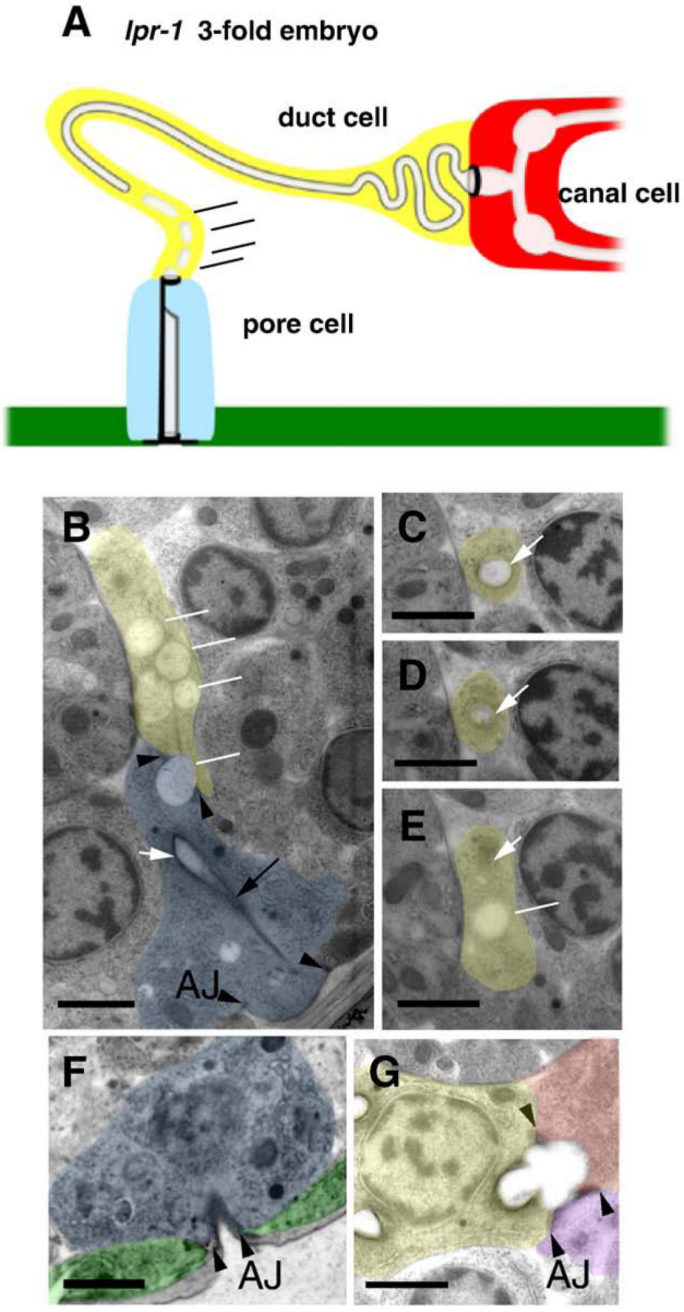

Fig. 6.

The duct and pore lumina are not connected in *lpr-1* mutants. (A) Schematic and (B–G) transmission electron micrographs of *lpr-1(cs73)* late 3-fold embryos. Canal cell, duct cell, pore cell, and ventral epithelium are colored red, yellow, blue, and green respectively. Lumen is uncolored and indicated by white arrows in TEMs. Black arrowheads indicate intercellular adherens junctions and black arrow indicates pore autocellular junction. Scale bars, 1 μm. (B) At the region of the duct–pore intercellular junction, the duct contains only disconnected vesicles (white lines), some of which appear to span the junction. (C–E) depict sequential sections of the duct cell process going from posterior to anterior, showing (C) normal lumen, (D) lumen terminating, and (E) lumen replaced by a disconnected vesicle. In

(E), white arrow indicates region where lumen should have been present and line indicates disconnected vesicle. The luminal cuticle of the duct and pore cells appears as a diffuse gray layer beneath a darker-staining plasma membrane in most specimens depending on section angle (panels C, D), but cuticle material is difficult to resolve inside the most disconnected vesicles. (F) The pore tube opens normally to the outside environment. (G) The canal cell and duct cell lumina are continuous through the secretory junction. Purple color indicates gland cell as in Fig. 1B.

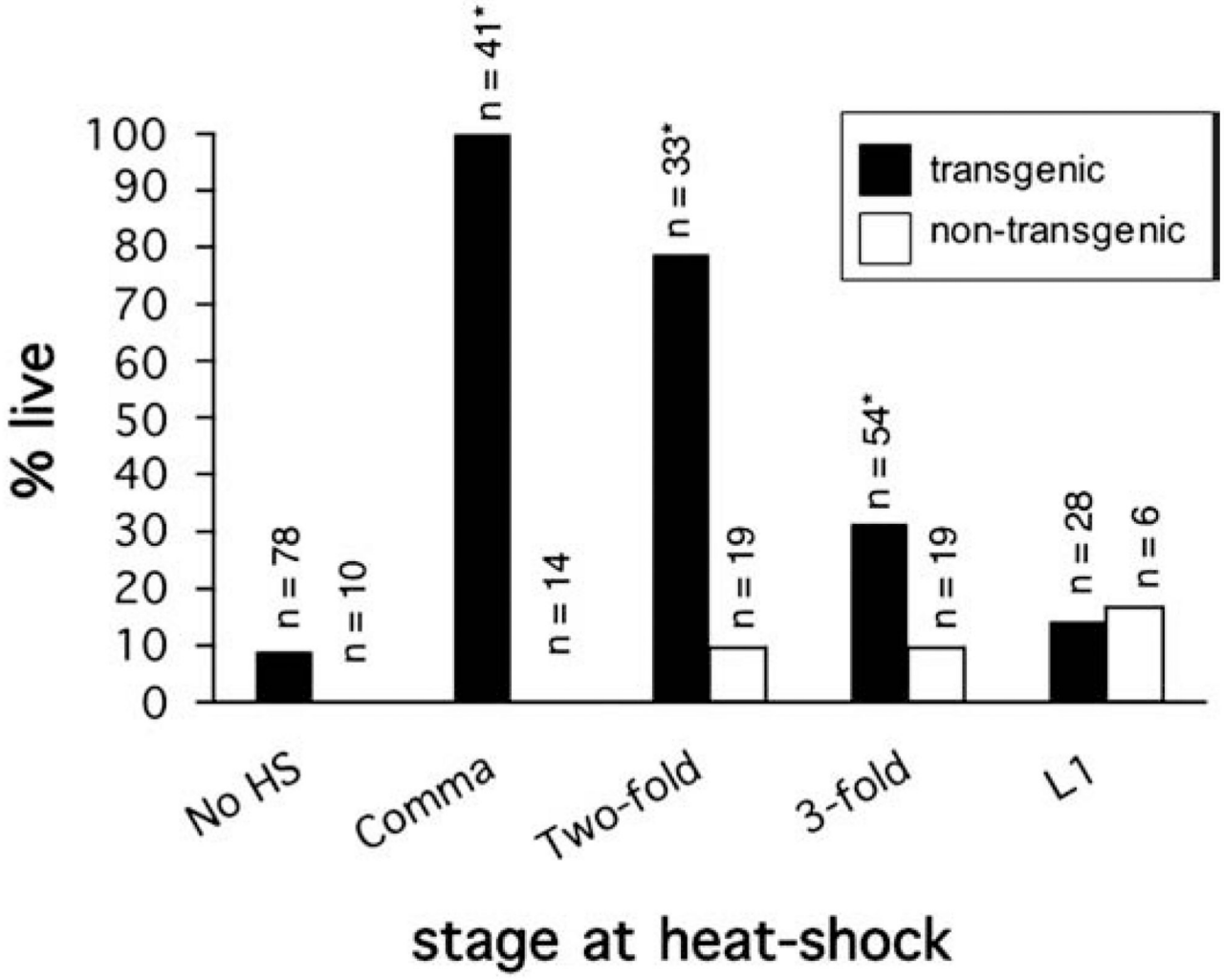

Fig. 7.

lpr-1 functions at the time of duct lumen outgrowth. Transgenic *lpr-1(cs73)*; *hsp16.2::lpr-1* mutant embryos grown at 15 °C were picked at the comma stage, and then incubated at 15 °C for an empirically determined amount of time prior to a 1-hour 35 °C heat-shock. L1s were picked and heat-shocked immediately after hatching. See Materials and methods for further details. Black bars indicate percent viability for transgenic animals, while white bars indicate percent viability for non-transgenic siblings. *p <0.01 (Fisher's Exact test) compared to non-heat-shocked controls.

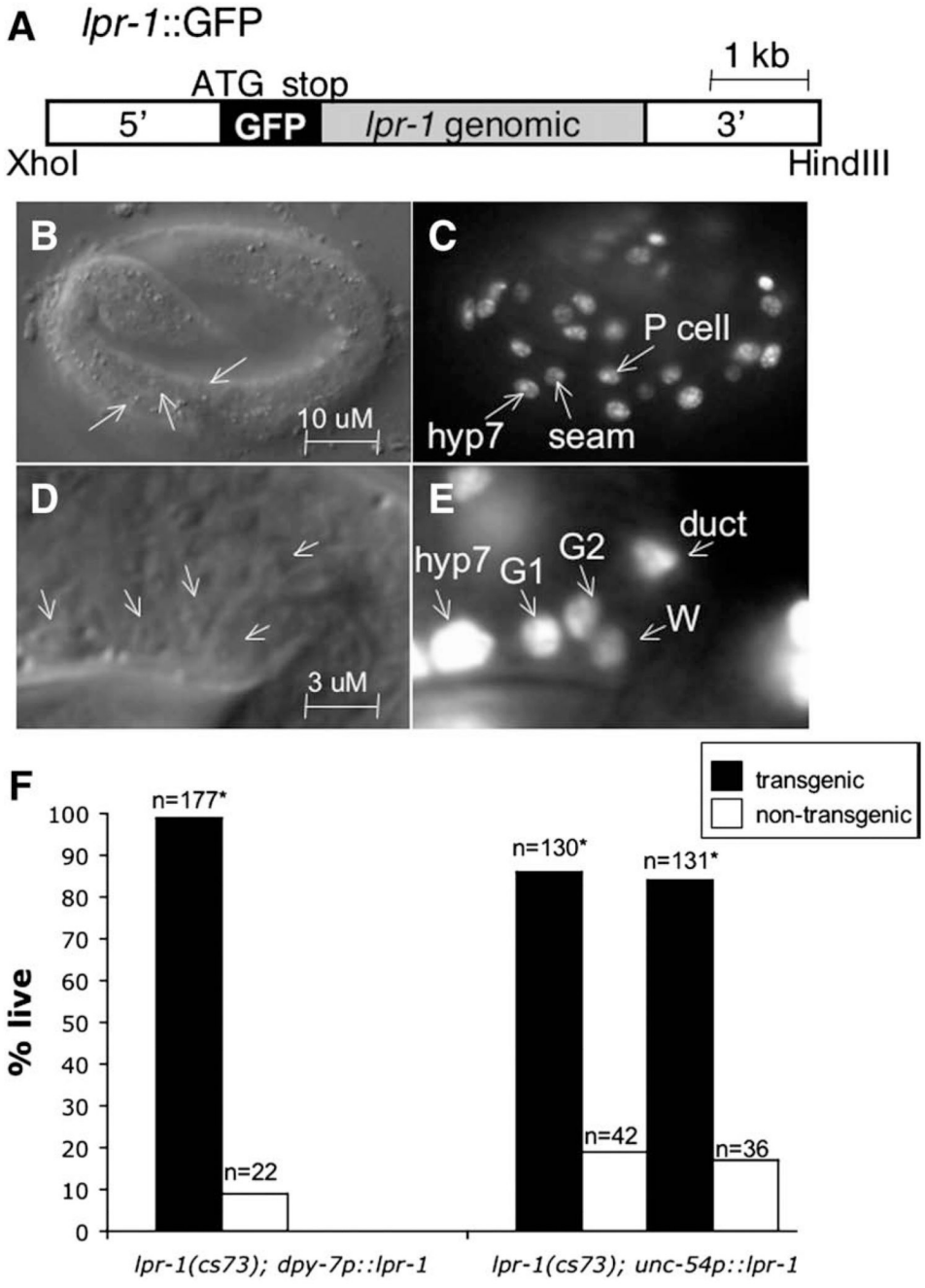

Fig. 8.

lpr-1 can function cell non-autonomously. (A) Schematic of the *lpr-1*::GFP transcriptional reporter. (B, C) *smg-1* 3-fold embryo expressing *lpr-1*::GFP in epidermal cell types (hyp7, P cells, seam cells). (D, E) Close-up view of the ventral head of a *smg-1* 3-fold embryo showing expression in the duct, G1 (embryonic and L1 pore), G2 (L2 pore and mother of L3-adult pore), and W (neuroblast and lineal homolog of G2). (F) *lpr-1a* was expressed under control of the tissue specific promoters *dpy-7* (epidermis) or *unc-54* (body wall muscle). The progeny of *lpr-1(cs73)* mutant animals bearing these transgenes were scored for viability to assess rescue (see Materials and methods). Results are shown for two independent lines carrying the *unc-54p::lpr-1a* transgene. Black bars indicate percent

viability for transgenic animals, while white bars indicate percent viability for non-transgenic siblings. *p <0.01 (Fisher's Exact test) compared to non-transgenic siblings.

Table 1

lpr-1 genetic analysis.

[i]Maternal genotype	% F1 lethal (*n*)
lpr-1(cs73)	94 (66)
lpr-1(cs73) 15 °C	95 (99)
lpr-1(cs73) 25 °C	98 (118)
[b]*lpr-1(cs73)*/+	16 (237)
+/*hDf10*	27 (120)
lpr-1(cs73)/hDf10	94 (151)
lpr-1(h276)	77 (92)
lpr-1(h276) 15 °C	95 (103)
lpr-1(h276) 25 °C	65 (186)
[c]*lpr-1(h276)*/+	35 (187)
[c]*lpr-1(h276)/hDf10*	92 (195)
[c]*lpr-1(cs73)/lpr-1(h276)*	91 (265)
[d]*lpr-1(cs73); csEx103*	17 (162)
[d]*lpr-1(h276); csEx103*	30 (215)
[d]*lpr-1(cs73); csEx104*	32 (115)
[d]*lpr-1(h276); csEx104*	42 (126)

[a] All data were collected at 20 °C unless otherwise noted.

[b] *lpr-1(cs73)* chromosome is marked with *unc-35(e259)*.

[c] *lpr-1(h276)* chromosome is marked with *dpy-5(e61)* and *unc-13(e450)*. This mutagenized chromosome has only been outcrossed once and may contain additional lesions, accounting for the higher than expected proportion of lethality seen in progeny of heterozygous mothers.

[d] *csEx103* and *csEx104* are extrachromosomal arrays containing *lpr-1* genomic rescue fragment pCS1 (see Fig. 4 and Materials and methods). The majority of F1 lethal progeny were non-transgenic as assessed by *unc-119::gfp* expression.

Table 2

Analyses of marker expression in *lpr-1* mutants.

Cell type	Marker	Stage	# Expressing marker/total		*lpr-1* Comments
			Wild-type	*lpr-1(cs73)*	
Canal cell	*vha-1*::GFP	3-fold embryos	ND	ND	*vha-1::gfp* expression is not completely penetrant until the mid-L1 stage. 29/29 *lpr-1(cs73)* GFP-expressing embryos had extended canals.
		L1[a]	34/45	22/44	All larvae have canal cell nucleus as judged by DIC. Canal processes are truncated and cystic.
Duct cell	*lin-48*::GFP	3-fold embryos	ND	ND	*lin-48::gfp* expression is not completely penetrant in the duct cell until the L1 stage
		L1[a]	32/34	57/59	
	lpr-1::GFP	3-fold embryos	8/9	10/10	
Pore cell	HMP-1::GFP	3-fold embryos	18/19	14/14	Duct process extends to pore cell
	lpr-1:GFP	3-fold embryos	7/9	10/10	
	AJM-1::GFP	3-fold embryos	16/16	12/12	Autocellular junction and junctions between cells appear normal
	HMP-1::GFP	3-fold embryos	19/19	14/14	
Canal-associated neurons	*ceh-23*:GFP	L1[a]	20/20	20/20	Axonal processes are short or absent, probably as secondary consequence of canal absence

[a]Newly hatched L1s were scored. For *lpr-1*, we scored only L1s with fluid accumulation.

Table 3

lpr-1(cs73) mutants are defective in phasmid DiO uptake.

Genotype	% amphid DiO uptake defective (*n*)	% phasmid DiO uptake defective (*n*)	# normal uptake	# uptake defective-1 phasmid	# uptake defective-2 phasmids
N2	0 (35)	0 (35)	35	0	0
lpr-1(cs73)	0 (17)	94 (17)	1	7	9

A dye uptake assay {Perkins et al., 1986 #240} was used to assess the integrity of the amphids, phasmids and their ensheathing channels. L4 larvae were incubated in DiO for 3 h and assessed for phasmid DiO uptake by epifluorescence. Rare, *lpr-1(cs73)* larvae that survived to the L4 stage were assayed.